Adsorbate Geometry Distinction in Arenethiols by Ion/Surface Reactive Collisions

T. Pradeep,*,† Chris Evans, Jianwei Shen, and R. Graham Cooks*

Department of Chemistry, Purdue University, West Lafayette, Indiana 47907

Received: January 27, 1999; In Final Form: April 16, 1999

Reactive scattering of low-energy ions from surfaces gives scattered product ions in which new bonds are formed with the adsorbate with a sensitivity to adsorbate geometry. Reactions of $Cr^{\bullet+}$ and $C_5H_5N^{\bullet+}$, as well as chemical sputtering induced by $Xe^{\bullet+}$, are used to distinguished two well-characterized monolayer systems, namely 1,4-benzenedimethanethiol (BDMT) adsorbed on Au(111) and Ag(111) thin films. While the reaction of $Cr^{\bullet+}$ with the Au monolayer produces an ion assigned as $CrC_7H_5S^+$, this product is completely absent upon reaction with the Ag monolayer. Pyridine ($C_5H_5N^{\bullet+}$) projectiles abstract C_1-C_8 hydrocarbon groups in 50 eV collisions with the Au monolayer, while the Ag monolayer shows only C_1-C_4 abstraction with a significantly different intensity pattern. Chemical sputtering ($Xe^{\bullet+}$) mass spectra of the two surfaces are substantially different; complete fragmentation of the Ag adsorbate occurs, leading to C_2-C_4 ion ejection, while more of the molecular features are preserved in the spectrum recorded for the Au monolayer. The experimental facts are interpreted in terms of the geometry of the BDMT molecule that is monocoordinated on Au and dicoordinated on Ag. The experiments are extended to the 1,2- and 1,3-ring isomers of 1,4-BDMT, which have not been characterized by other forms of surface spectroscopy. Ion/surface reactive collisions are useful for characterizing chemisorbates, including their geometrical orientation.

Introduction

Ionic reactions at molecular surfaces form a topic of considerable current interest.[1−4] The diversity of the chemistry,[4] its implications for materials design,[5] and the technological applications of surface transformations[6] are all important. Investigation of ion/surface collisions[7−10] and increased understanding of the molecular details of the processes by performing analogous ion/molecule collisions[8,11] have widened the scope of this area. Ions at low energies interact only with the first few atomic layers of a surface[12] and reactions appear to be limited to the topmost atomic layers.[13] These characteristics make reactive collisions of interest as a tool for surface analysis and modification. To identify surface species, systematic information on the behavior of different types of ionic reagents is needed for different surfaces. In this study, the scope of ion/surface reactive collisions is extended to cover variations in the geometry of the adsorbate. The ion beam acts as a chemical reagent in ion/surface collisions, and the processes observed are therefore expected to be sensitive to the orientation of the adsorbate. Careful experiments have already been devised to show that geometric effects are manifest in the scattered ion beam. Studies and molecular dynamics simulations have investigated the surface's role in the kinetic energy of the scattered ion beam resulting from changes in the self-assembled monolayer terminal group.[14−16] Surface-induced dissociation processes and hydrogen abstraction reactions are surface-monolayer specific and thus can be employed to monitor the condition of self-assembled monolayer surfaces as well as to explore chain length effects on chain terminus orientation.[17]

Self-assembled monolayers (SAMs) are widely used for the investigation of surface chemical and physical properties[18,19] and have potential applications in microelectronic device fabrication.[20,21] One major reason for the widespread use of SAMs as collision partners in low-energy ion/surface collision studies is their low tendency to adsorb contaminants.[22,23] This makes self-assembled monolayers suitable systems for distinguishing adsorbate geometry differences. In this study, self-assembled monolayers of 1,2-, 1,3-, and 1,4-benzenedimethanethiol (1,4-BDMT) on gold and silver are used as target surfaces to seek differences due to the geometry of adsorption upon reactive ion scattering. Previous independent experiments have investigated the adsorbate geometries of 1,4-BDMT on both gold and silver.[24] These studies showed that the molecule adsorbs dissociatively on both gold and silver, creating SAMs with the thiolate structure. Whereas two thiol protons are lost upon adsorption on Ag, only one is lost when adsorbed on Au. As a result of this adsorption, the molecular plane is parallel to the surface on Ag and perpendicular on Au with one thiol group projecting up at the monolayer vacuum interface. In surface-enhanced Raman spectroscopy (SERS), the difference in adsorption geometry is manifested as the presence of aromatic C−H and S−H stretches and an S−C−H bend from the Au monolayer and the complete absence of these in the Ag monolayer.

Experimental Section

Monolayer surfaces were prepared on gold that had been vapor deposited (2000 Å) on optically polished silicon wafers and on silver (2000 Å) deposited optically on polished glass plates, both metals being bound to the substrate by a 50 Å Cr adhesion layer. The X-ray diffraction patterns (Siemens diffractometer, Cu Kα radiation) of both substrates showed only (111) reflections, in agreement with the fact that thin film growth occurs along the low-energy plane. The surfaces were cleaned with piranha solution (concentrated H_2SO_4 and 30% H_2O_2, in 3:1 volume ratio, heated to 100 °C) before exposure to the thiol

* To whom correspondence should be addressed.

† Fulbright Fellow, on leave from the Department of Chemistry and Regional Sophisticated Instrumentation Centre, Indian Institute of Technology, Madras 600 036, India.

10.1021/jp9903099 CCC: $18.00
Published on Web 06/06/1999

(caution: piranha solution is highly oxidizing and care should be taken in handling it). The resulting monolayers were prepared by the well-documented procedure[25] of exposing a 1 mM solution of the corresponding thiol in ethyl alcohol to previously cleaned surfaces for 24 h. After exposure, the surfaces were washed with ethanol repeatedly and dried in a stream of nitrogen and inserted into the spectrometer. XPS analysis (Physical Electronics, Mg Kα nonmonochromatic radiation, 70 mW) of these monolayers showed no adventitious species.

Experiments were conducted using a four-analyzer BEEQ mass spectrometer described previously.[26] A mass- and energy-analyzed ion beam was directed at the surface held in an ultrahigh vacuum scattering chamber. The beam was decelerated and brought to the set collision energy prior to surface impact. The energy and mass distribution of the product ions was analyzed using the remaining EQ analyzers. In the experiments described below, the incident angle was 45° and the scattering angle was set at 90°. The experiments were conducted at a base vacuum of 2×10^{-9} Torr and chemical sputtering experiments showed negligible adventitious carbonaceous species on the surface. Under these vacuum conditions, adventitious contaminants are not observed on hydrocarbon SAMs for the first few hours after introduction. The collision energy range investigated was 10−90 eV. Primary ions were generated by 70 eV electron impact. All data are recorded in Thomson, where 1 Th = 1 Da/electronic charge,[27] in low-resolution mode ($\Delta m = 2$ Da, at half-height) due to the low abundance of the scattered ions. Typical ion/surface measurement periods were less than 1 h, and the ion doses involved were approximately 10^{10} (ion/cm^2)/s. Over the measurement period, significant surface damage is not expected.[17] In agreement with this expectation, no time dependent effects were seen. Different monolayers were used for each series of experiments.

Results and Discussion

Ion/Surface Reactions and Chemical Sputtering. Scattered ion mass spectra recorded upon collision of 90 eV $^{52}Cr^{\bullet+}$ ions at 1,4-BDMT monolayers chemisorbed on Au and Ag are shown in Figure 1. A large fraction of the ion current is lost due to neutralization at the surfaces. Principal features of interest are the differences that occur in both the high- and low-mass regions between the two monolayer surfaces. In the case of the monolayer assembled on Au, ions up to *m*/*z* 173 are observed, whereas for the Ag case, there is no prominent peak above *m*/*z* 52. In both experiments, the major ion scattered from the surface is the reflected Cr^+ projectile ion. Either the remaining ions originate from the surface, and correspond to surface molecular fragments emitted in the process known as chemical sputtering,[28] or they are ionic products of bond-forming reactions between the adsorbate and the projectile. In the case of the monolayer assembled on Ag, the most prominent peaks are due to hydrocarbon ions resulting from chemical sputtering of the adsorbed species. Peaks corresponding to C_2 and C_3 hydrocarbon species are observed in greater abundance than the C_4 hydrocarbon species. In the case of the monolayer assembled on Au, the $Cr^{\bullet+}$ spectrum is characterized by a series of peaks that correspond to C_2 to C_8 hydrocarbon ions, the higher mass ions being more weakly represented. While giving a major signal in the case of the Au monolayer surface, the C_5 hydrocarbon ions are completely absent for the Ag monolayer surface. Particularly interesting is the peak at *m*/*z* 173, shown by isotopic selection to contain Cr (see the inset of Figure 1). This ion is present in the spectrum of the adsorbate on Au but absent in the Ag surface experiment. We assign the peak to the ion, $(SCH-C_6H_4)-Cr^+$,

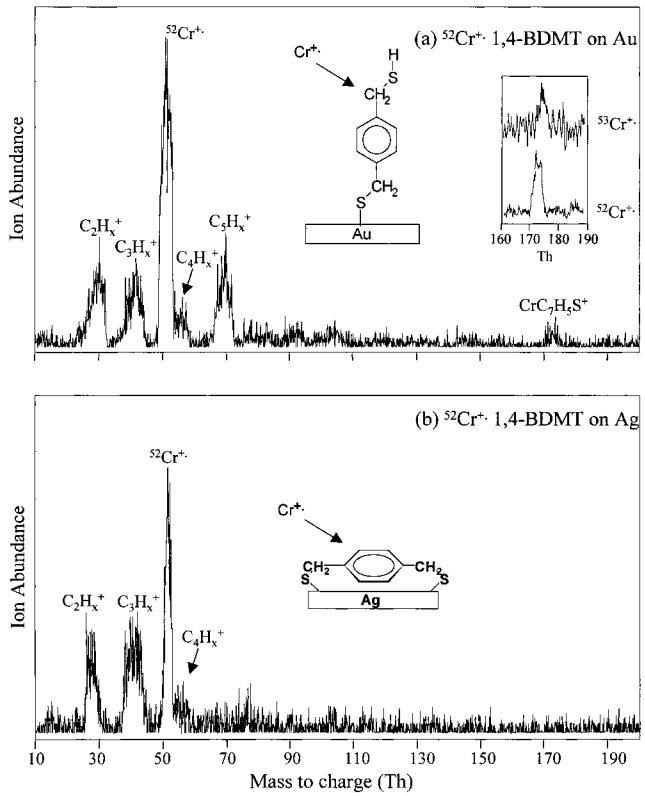

Figure 1. Scattered ion mass spectra recorded upon collision of 90 eV $Cr^{\bullet+}$ ions on 1,4-BDMT monolayers assembled on (a) Au and (b) Ag. Assignments are suggested for the prominent peaks. Note the peak at *m*/*z* 173.

the structure of which is not known or is not of immediate concern. Of interest, however, is the fact that the adsorbate geometry at Au is such that abstraction of a major portion of the adsorbate is possible, while similar behavior is not observed for chemisorption of 1,4-DBMT on Ag.

Scattering of 50 eV pyridine molecular ions, $C_5H_5N^{\bullet+}$ (*m*/*z* 79), from the monolayer of 1,4-BDMT on Au, is compared in Figure 2 to the behavior of its positional isomers. Analogously, Figure 3 shows the corresponding data for the 1,4-BDMT monolayer on Ag in comparison with the data for its ring-substituted isomers. The ion/surface collisions lead to fragmentation of the pyridine projectile, and the most abundant peaks below *m*/*z* 79, mainly *m*/*z* 26 and 27 and *m*/*z* 52 and 53 are attributed simply to surface-induced dissociation (Figures 2 and 3). This is consistent with previously reported data[1,29] on dissociative scattering of pyridine molecular ions at hydrocarbon surfaces. As can be seen, there are significant differences in the product ions at higher masses when the Au and Ag surfaces are compared. The peaks above *m*/*z* 79, which are spaced by approximately 14 Th, are consistent with hydrocarbon additions to the pyridine projectile ion. The exact chemical composition of these peaks is not known. Spectra collected at lower energy (20−30 eV), however, confirmed addition of C_1 and C_2 groups to the pyridine projectile ion. During collisions at 50 eV, as shown in Figures 2 and 3, other processes may contribute to the abundance of the peaks present above *m*/*z* 79. At this energy chemical sputtering is likely to be an important process. The peaks observed at *m*/*z* 91, from both monolayers, may result from both chemical sputtering of surface-bound species to form $C_7H_7^+$, as well as from hydrocarbon abstraction by the pyridine projectile ions to form $[C_6H_5N]-CH_2^{\bullet+}$. At lower energy collisions, where chemical sputtering is not a dominant process, hydrocarbon abstraction is still observed. In addition to the C_nH_m

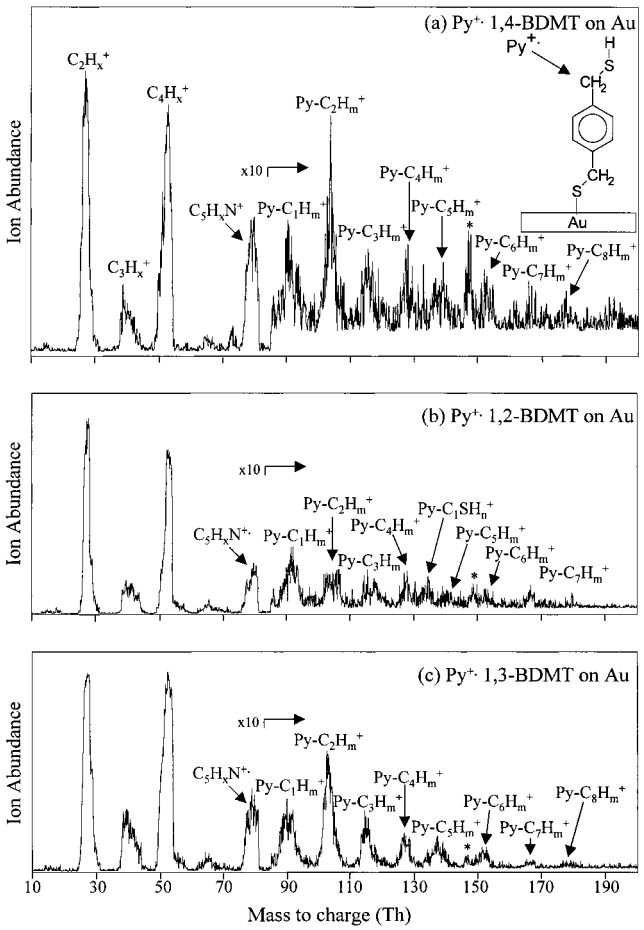

Figure 2. Scattered ion mass spectra recorded upon collision of 50 eV $C_5H_5N^{\bullet+}$ ions on (a) 1,4-BDMT, (b) 1,2-BDMT, and (c) 1,3-BDMT assembled on Au. Note the pickup of hydrocarbon fragments. Assignments are suggested for the prominent peaks. The peak marked * is due to phthalate contamination.

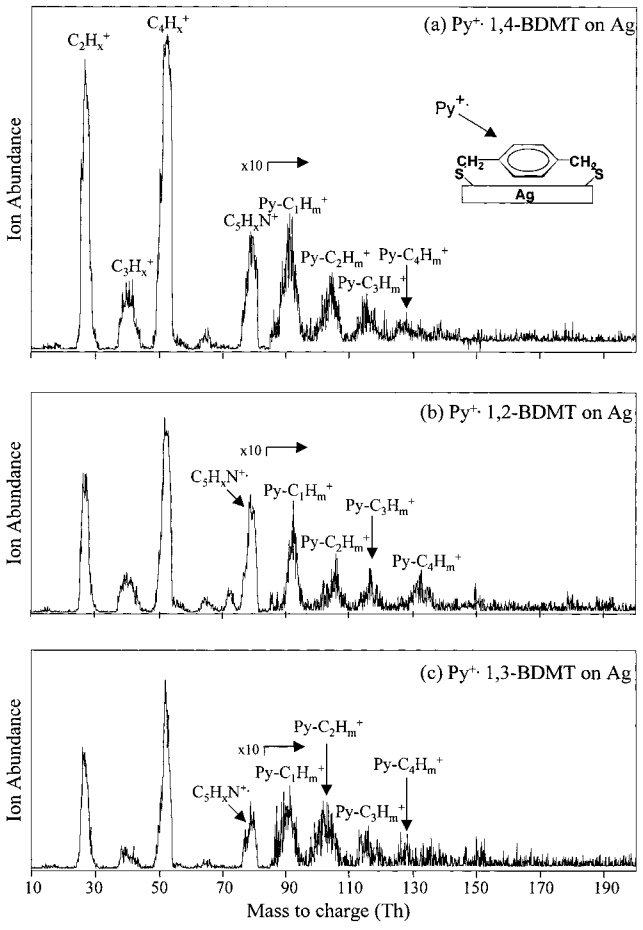

Figure 3. Scattered ion mass spectra recorded upon collision of 50 eV $C_5H_5N^{\bullet+}$ ions on (a) 1,4-BDMT, (b) 1,2-BDMT, and (c) 1,3-BDMT assembled on Ag. Again, note the pickup of hydrocarbon fragments. Assignments are suggested for the prominent peaks.

abstractions, the 1,2-BDMT monolayer on Au also appears to show contributions from C_nSH_m ions. The isomeric BDMT chemisorbates on Au each display a maximum of eight carbon atom abstractions, whereas when they are assembled on Ag, abstraction of hydrocarbon groups with a maximum of four carbons by pyridine is observed. The intensity of the peaks due to these pickup reactions gradually decreases to higher mass. When comparing the abstraction patterns from the three Ag surfaces are compared to the abstractions observed from the corresponding Au surfaces shown in Figure 2, there are clear differences. The important result is that the two substrates are readily distinguished in the case of each of the three isomers even though the chemical composition of many of the peaks is not verifiable. For the Au surfaces, peaks consistent with the additions of fragments with up to eight carbons are observed, while for Ag, groups containing a maximum of five carbon atoms are picked up by the reacting ion.

Figure 4 shows the scattered ion mass spectrum recorded upon collision of $Xe^{\bullet+}$ with the 1,4-BDMT monolayer on Au at 90 eV collision energy and compares this with the spectra of the 1,2- and 1,3-BDMT isomers. The corresponding data for the BDMT monolayers on Ag are shown in Figure 5. As in the case of $Cr^{\bullet+}$ collisions, the Ag monolayer spectra show mainly peaks in the low-mass region while for the Au chemisorbate, peaks with significant intensities are observed at higher masses. Again, the abundant peaks noted in the low-mass region are due to chemical sputtering of the adsorbate. Of particular interest are the ions at *m*/*z* 90, 104, and 135. Which are weak or absent for the isomeric BDMT monolayers on Ag, while considerably more abundant in the case of these monolayers assembled on Au. They are assigned as $C_6H_4-CH_2^+$, $CH_2-C_6H_4-CH_2^+$, and $^+CH_2-C_6H_4-CH-S$, respectively. In the case of the 1,2-BDMT monolayer on Au, comparable peaks are observed at *m*/*z* 90 and 104, but a very intense peak at *m*/*z* 135 is also observed. Similarities between the 1,4- and 1,3-BDMT chemical sputtering mass spectra on Au and Ag (as shown in Figure 5) point to similar adsorbate structures, while the ortho isomer behaves distinctively. One characteristic feature of the 1,2-BDMT on Ag spectrum is the abundant ion at *m*/*z* 18 due to $H_2O^{\bullet+}$. This might be due to intercalated H_2O or to defects in the monolayer, although there is no other evidence for this. Second, a strong peak at *m*/*z* 135, again assigned to $^+CH_2-C_6H_4-CHS$ is observed only for the 1,2-BDMT isomer on Ag. Table 1 summarizes the most important scattered ion products from the ion/surface reactions and chemical sputtering processes.

Interpretation of 1,4-BDMT Data. On the basis of independent data[24] we propose that, when the 1,4-BDMT molecule is self-assembled on Au, only one sulfur is bound to the surface, thus making it possible to cleave a single bond and abstract the $HS-CH_2-C_6H_4^-$ group; this ion is suggested to subsequently lose H_2, forming the species at *m*/*z* 173. Cleavage of the $C_6H_4-CH_2$ bond is energetically unfavorable compared to cleavage of the CH_2-S bond; however, this is compensated for by the stability of the C_7 cyclic ion (substituted tropylium or benzyl) that can be formed in this case. When 1,4-BDMT is assembled on Ag, the spectra are interpreted in terms of an adsorbate

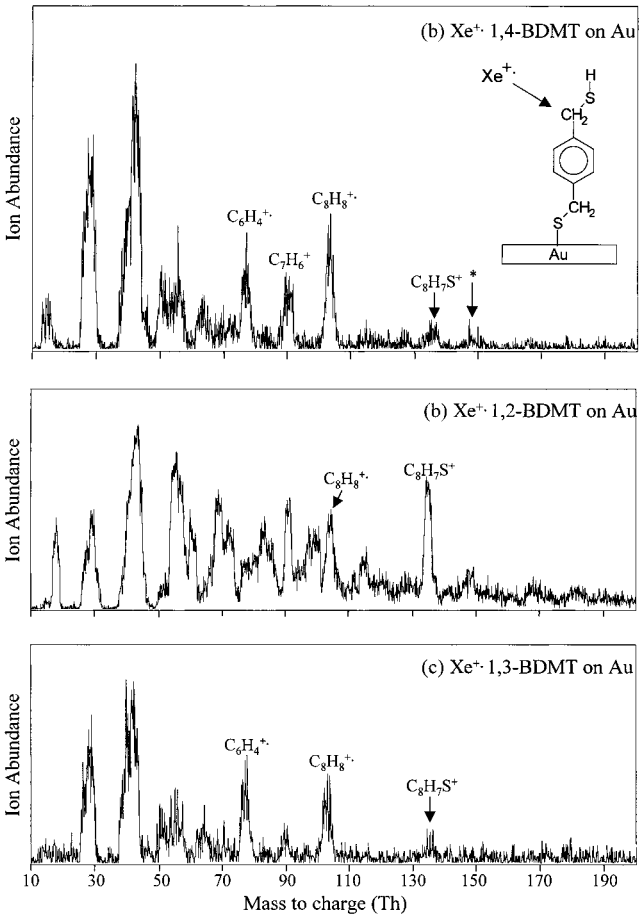

Figure 4. Scattered ion mass spectra recorded upon collision of 90 eV $Xe^{\bullet+}$ ions on (a) 1,4-BDMT, (b) 1,2-BDMT, and (c) 1,3-BDMT assembled on Au. Note the peaks at *m*/*z* 90, 104, and 135. Assignments are suggested for the prominent peaks. The peak marked * is due to phthalate contamination.

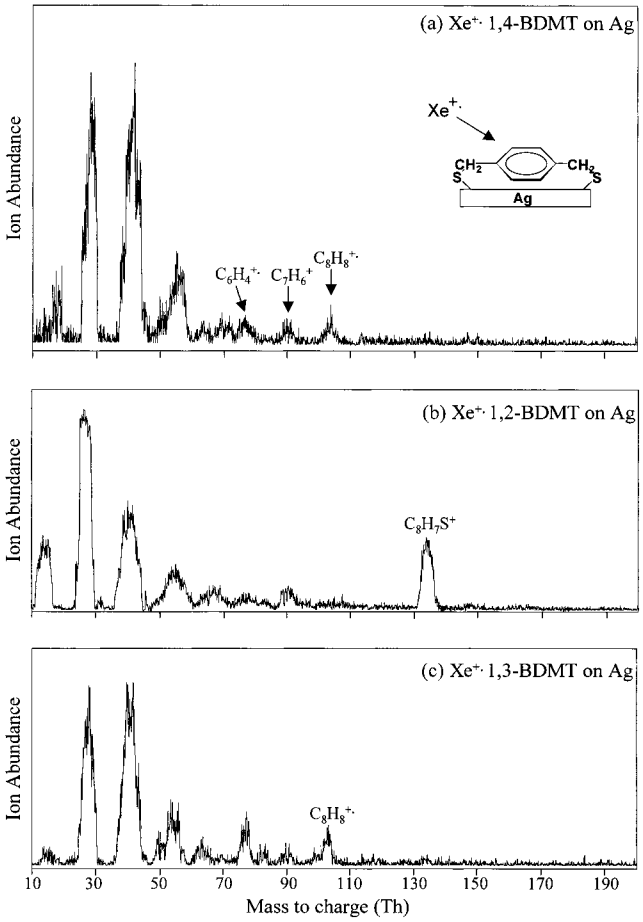

Figure 5. Scattered ion mass spectra recorded upon collision of 90 eV $Xe^{\bullet+}$ ions on (a) 1,4-BDMT, (b) 1,2-BDMT, and (c) 1,3-BDMT assembled on Ag. Note the peaks at *m*/*z* 90, 104, and 135. Assignments are suggested for the prominent peaks.

structure in which both thiols of the 1,4-BDMT molecule are bound to the surface. In this bidentate form, there is probably an increased interaction with the surface due to ring−surface π bonding. Both these aspects would mitigate against formation of the ion at *m*/*z* 173 in this case, even though the Ag−S bond energy of 51.9 kcal/mol is significantly lower than the Au−S bond energy of 100 kcal/mol.[30] The energy dependence of the reaction leading to *m*/*z* 173 was studied for the gold surface and an approximate onset of 50 eV lab collision energy determined. This is consistent[31] with cleavage of a relatively strong aryl−CH_2 bond. Another notable difference between the two spectra (Figure 1) is the larger absolute signal (and relatively smaller noise) resulting from the collision of $Cr^{\bullet+}$ with the Au surface as compared to the Ag surface. This effect is explained as a consequence of the proposed mono- vs bidentate bonding in the Au vs the Ag case.

Although the pickup of a group containing one to four carbon atoms from hydrocarbon surfaces by pyridine molecular ions has been reported previously,[1] C_6H_n is the heaviest carbon species abstracted by polycyclic aromatic hydrocarbon ions from hydrocarbon-covered surfaces.[32] The abstraction of up to eight carbon species from an adsorbate by a monocyclic ion is therefore noteworthy. Previous studies have shown pyridine molecular ions to undergo C_1 and C_2 abstraction reactions by formation of a new bond formed to the nitrogen atom.[33] As the number of carbon atoms abstracted increases, the width of the observed mass peak increases due to the presence of multiple hydrogen atoms.

Abstraction of heavier hydrocarbon fragments is more likely in the case of the Au adsorbate where cleavage of one Au−S bond can potentially abstract up to eight carbon atoms. In the case of Ag, both Ag−S bonds must be cleaved for the abstraction of all eight carbon atoms. This is a less probable process and abstraction of fragments rather than the complete adsorbate is expected to be favored, as observed.

The experimental facts presented above establish that there is considerable difference in the ion/surface chemistry between the 1,4-BDMT in the two different adsorbate geometries. The difference is expected, considering the surface specificity of low-energy ion/surface collisions. Even in SIMS, at 1.5 keV primary ion energy, most of the ejected material comes from the first two atomic layers,[12] and at energies below 100 eV, the released ions are derived exclusively from the topmost atomic layers.[13] Molecular dynamics simulations of particle collisions at surfaces have also shown that the region of interaction is limited to the first few atomic layers.[16,34] The experimental observations can be rationalized on the basis of the limited penetration depth (of ions that retain sufficient energy to be scattered) and the adsorption geometry. During projectile ion collisions at the monolayer assembled on Ag (see the schematic included in Figure 5), the phenyl ring is more exposed to ion impact, making ring as opposed to substituent bond cleavage more likely.

The above conclusions are based on and consistent with what is known from independent experiments about the adsorbate geometries of 1,4-BDMT on both gold and silver. These surfaces have previously been studied with surface-enhanced Raman spectroscopy (SERS) and X-ray photoelectron spectroscopy

TABLE 1: Most Important Observed Scattered Ion Products from Ion/Surface Reactions and Chemical Sputtering Processes That Are Used To Differentiate the Geometric Differences between the Monolayers

	ion projectile		
	$^{52}Cr^{\bullet+}$	pyridine ($Py^{\bullet+}$)	$Xe^{\bullet+}$
1,4-BDMT on Au	ions observed up to and including *m*/*z* 173 $(CrC_7H_5S)^+$	abstraction of up to eight carbon-containing species	high-mass ions observed, including *m*/*z* 90, 104, and 135 ($C_6H_4-CH_2^+$, $CH_2-C_6H_4-CH_2$, and $CH_2-C_6H_4-CH-S^+$)
Ag	no ions observed above *m*/*z* 52	abstraction of up to only four to five carbon-containing species	ions observed at *m*/*z* 90 and 104, while no ions observed at *m*/*z* 135
1,3-BDMT on Au		abstraction of up to eight carbon-containing species	high-mass ions observed, including *m*/*z* 90, 104, and 135 ($C_6H_4-CH_2^+$, $CH_2-C_6H_4-CH_2^+$, and $CH_2-C_6H_4-CH-S^+$)
Ag		abstraction of up to only four to five carbon-containing species	ions observed at *m*/*z* 90 and 104, while no ions observed at *m*/*z* 135
1,2-BDMT on Au		abstraction of up to eight carbon-containing species	high-mass ions observed, including *m*/*z* 90 and 104 ($C_6H_4-CH_2^+$ and $CH_2-C_6H_4-CH_2^+$) very intense peak at *m*/*z* 135 ($CH_2-C_6H_4-CH-S^+$) due to the "ortho effect"
Ag		abstraction of up to only four to five carbon-containing species	ions observed at *m*/*z* 90 and 104 very intense peak at *m*/*z* 135 due to the "ortho effect"

(XPS). As discussed previously, when 1,4-BDMT is assembled on Au, it binds through one thiol group, losing a proton, while the other thiol projects up at the monolayer−vacuum interface.[24] By contrast, when assembled on Ag, the 1,4-BDMT molecule binds through both thiol groups in the bis-thiolate form.[24] Adsorption geometries of the ring isomers, namely, 1,2- and 1,3-BDMT, have not been investigated by other spectroscopic methods.

Earlier studies have shown that alkanethiolate SAMs organize differently on Ag(111) than on Au(111). While Au(111) has a $(v3 \times v3)R30°$ overlayer orientation, it is reported to be $(v7 \times v7)$ on Ag (111).[23] These differences in overlayer orientation between the two crystal structures cause compounds to adsorb differently. These surface structures, although determined for alkanethiolate SAMs, can serve as model systems for aromatic thiol systems investigated here. Top and 3-fold hollow sites (or a combination) of the crystal may be utilized for SAM adsorption, thus providing numerous geometric adsorption possibilities for systems with multiple anchoring groups. For instance, the distance between the two sulfur atoms in the dithiolate form of 1,4-BDMT is nearly 8.4 Å, quite close to the near-neighbor hollow sites located 8.834 Å apart for Ag.[25] This spacing allows multiple attachments to the Ag surface, and by occupying two such sites, the 1,4-BDMT molecule is observed to "lie down", or adopt a parallel orientation to the Ag surface. Note that this conclusion is based on the assumption that the BDMT self-assembled monolayers in this study do not adsorb to the Au and Ag surfaces, rather they assemble in a fashion similar to alkanethiolate self-assembled monolayers. Monolayer surfaces were prepared on optically smooth gold and silver that had been vapor deposited on polished silicon wafers and glass substrates, while the SERS study investigating the adsorption geometry of 1,4-BDMT was completed on SERS-active submicron roughened surfaces. No difference in adsorption geometry is expected from this SERS activation of the substrate.

Interpretation of 1,2- and 1,3-BDMT Data. Comparison of mass spectra collected from ion/surface collisions with the ring isomers of BDMT having an unknown adsorption geometry, and mass spectra collected from ion/surface collisions with 1,4-BDMT, with previously characterized adsorption geometries, allows several conclusions to be drawn about adsorption geometry. First, it is probable that 1,2-BDMT adsorbs to both Au and Ag surfaces through only one thiol. Direct evidence for this is the intense peak at *m*/*z* 135 observed in the chemical sputtering mass spectra recorded for both surfaces, as shown in Figures 4b and 5b. The enhancement of the *m*/*z* 135 peak, as

SCHEME 1: Proposed Mechanism To Explain the Enhanced Abundance of the Peak at *m*/*z* 135, Observed from $Xe^{\bullet+}$ Collisions with a 1,2-BDMT Monolayer Assembly on Both Au and Ag Surfaces

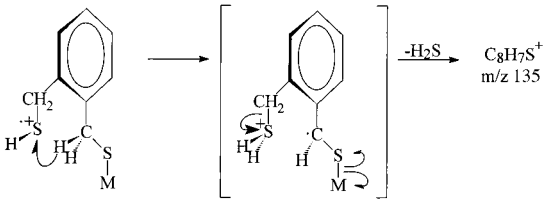

compared to its abundance in 1,3- and 1,4-BDMT monolayers, is suggested to be due to an ortho effect, illustrated in Scheme 1. Formation of this ion follows proton transfer and release of the surface-bound species accompanied by neutral H_2S loss. This mechanism requires the ortho orientation of the carbon chains. In addition, spectra collected from collisions of pyridine molecular ions with the monolayer assembled on Au show abstraction of fragments up to C_8, consistent with the number of carbon atoms in the groups abstracted from 1,4-BDMT on Au where there is independent evidence for adsorption through one thiol. By contrast, when assembled on Ag, the fragments abstracted consist of up to C_4 species only. While it is bound by only one thiol, as suggested by the intense peak at *m*/*z* 135, π interactions of the ring with the Ag surface may cause the ring to adopt a near parallel orientation to the surface. Such an orientation would inhibit the abstraction of large fragments of the adsorbate by the pyridine molecular ion, as in the 1,4-BDMT monolayer on Ag, where independent evidence gathered from surfaced-enhanced Raman scattering shows the ring to be oriented parallel to the surface.[24]

Spectra collected from ion/surface collisions with the 1,3-BDMT monolayer indicate that 1,3-BDMT monolayers adsorbed on Au are bound through one thiol, as in the case of 1,4-BDMT monolayers on Au. Reactive ion collisions of pyridine molecular ions (Figure 2c) show that pickup of groups containing a maximum of eight carbons occurs in ion/surface collisions with 1,3-BDMT on Au, just as with 1,4-BDMT where adsorption is through one thiol. Chemical sputtering mass spectra (Figure 4c) collected from $Xe^{\bullet+}$ collisions with 1,3-BDMT on Au, also give very similar data to 1,4-BDMT on Au with respect to the ions observed at *m*/*z* 76, 90, 104, and 135. Such similarities in the spectra again indicate that 1,3-BDMT monolayers on Au are bound through one thiol.

Spectra collected from ion/surface collisions with 1,3-BDMT monolayers on Ag indicate that this species is most likely bound

to the surface through both thiol groups and probably adopts a near parallel orientation to the Ag surface. Reactive ion collisions of pyridine molecular ions with the monolayer assembled on Ag (Figure 3c) show abstraction of up to C_4 species only, consistent with the number of abstractions from 1,4-BDMT on Ag where adsorption occurs through both thiols and the ring is oriented parallel to the Ag surface. In addition, chemical sputtering mass spectra (Figure 5c) are consistent with spectra collected from analogous collisions with 1,4-BDMT monolayers on Ag, namely the ions at *m*/*z* 76, 90, and 104 are of low abundance, and no enhancement of *m*/*z* 135 occurs.

Conclusions

Ion/surface reactive collisions and charge exchange leading to chemical sputtering are both sensitive to chemisorbate geometry in the substituted aromatic compounds studied. Reactions of the pyridine molecular ion lead to the pickup of large parts of the adsorbate molecule from monolayers of 1,4-BDMT on Au, whereas monolayers of 1,4-BDMT on Ag allow only a small portions of the molecule to be abstracted. Adsorbate geometry also influences the reactions of metal ions, and a pickup reaction of the adsorbate-derived group, C_7H_5S, by $Cr^{\bullet+}$ is observed from monolayers of 1,4-BDMT supported on Au, while chemisorption of the same compound on Ag leads to no such reaction. The differences in adsorbate geometry are also manifest in the chemical sputtering spectra, which can also be used to distinguish disorder in the adsorbate by allowing detection of trace quantities of adventitious species. In the case of fully organized structures, ions due to contaminants are not observed and this was the case with the surfaces studied here with the possible exception of 1,2-BDMT on Ag. Collectively, the data summarized in Table 1 are interpreted as being consistent with the suggestion made in ref 24 that monolayers of 1,4-BDMT are assembled on Au by binding to the surface through only one thiol, whereas in monolayers of 1,4-BDMT assembled on Ag the adsorbate is bound through both thiols.

On the basis of the information derived from the independently characterized 1,4-BDMT adsorbate systems, the adsorbate geometry of related systems is inferred. Ion/surface collisions involving the ring isomers, 1,2- and 1,3-BDMT on Au and Ag, allow conclusions to be drawn about their adsorption geometry. Monolayers of 1,2- and 1,3-BDMT, when assembled on Au surfaces, orient themselves perpendicularly to the surface and bind to the Au through only one of the thiol groups, with the second thiol projecting upward at the monolayer−vacuum interface. Monolayers of 1,3-BDMT assemble on Ag in a manner such that the ring structure is bound to the Ag surface through both thiol groups, causing the molecule to lie flat on the Ag surface. While 1,2-BDMT appears to adsorb to Ag surfaces through only one thiol group, π interactions of the ring with the Ag surface may result in a near parallel ring orientation to the surface in this case.

The study also suggests that the ion/surface reactions of interest here occur *at* the surface and not *above* the surface where gas-phase ion/molecule association processes would be involved.[35] This conclusion comes from fact that the chemical sputtering spectra yield distinctive ions, which are not those involved in the pyridine or $Cr^{\bullet+}$ ion/surface reactions.

The demonstration that adsorbate geometry of monomolecular films can be characterized, even to a limited extent, by ion/surface collisions may represent a significant development that complements the well-established analysis of surfaces using kiloelectronvolt energy ion beams.[36,37] The discovery of ion/surface reactions that are sensitive to closely related chemical species should make it possible to extend the scope of this methodology for adsorbate characterization. The fact that ion/surface inelastic processes can provide data even for fractional monolayer coverages should increase the potential value of this approach.

Acknowledgment. This work was supported by National Science Foundation (CHE-9732670). T.P. acknowledges the award of a Fulbright Fellowship and a Fulbright-Tata travel grant.

References and Notes

(1) Cooks, R. G.; Ast, T.; Mabud, M. A. *Int. J. Mass Spectrom. Ion Processes* **1990**, *100*, 209.
(2) Wörgötter, R.; Grill, V.; Herman, Z.; Schwarz, H.; Märk, T. D. *Chem. Phys. Lett.* **1997**, *270*, 333.
(3) Wörgötter, R.; Kubista, J.; Zabka, J.; Dolejsek, Z.; Märk, T. D.; Herman, Z. *Int. J. Mass Spectrom. Ion Processes* **1998**, *174*, 53.
(4) Cooks, R. G.; Ast, T.; Pradeep, T.; Wysocki, V. H. *Acc. Chem. Res.* **1994**, *27*, 316.
(5) Miller, S. A.; Luo, H.; Pachuta, S. J.; Cooks, R. G. *Science* **1997**, *275*, 1447. Compare with: Ceyer, S. T. *Annu. Rev. Phys. Chem.* **1988**, *39*, 479.
(6) Shi, J.; Kikawa, J. M.; Proksch R.; Schaffer, T.; Awschalom, D. D.; Medeirosribeiro, G.; Petroff, P. M. *Nature* **1995**, *377*, 707.
(7) Ada, E. T.; Kornienko, O.; Hanley, L. *J. Phys. Chem. B* **1998**, *102*, 3959.
(8) Hayward, M. J.; Park, F. D. S.; Phelan, L. M.; Bernasek, S. L.; Somogyi, A.; Wysocki, V. H. *J. Am. Chem. Soc.* **1996**, *118*, 8375.
(9) Koppers, W. R.; Beijersbergen, J. H. M.; Weeding, T. L.; Kistemaker, P. G.; Kleyn, A. W. *J. Chem. Phys.* **1997**, *107*, 10736.
(10) Morris, J. R.; Kim, G.; Barstis, T. L. O.; Mitra, R.; Jacobs, D. C. *J. Chem. Phys.* **1997**, *107*, 6448.
(11) Pradeep, T.; Riederer, D. E., Jr.; Hoke, S. H.; Ast, T.; Cooks, R. G.; Linford, M. R. *J. Am. Chem. Soc.* **1994**, *116*, 8658.
(12) In SIMS, even at kiloelectronvolt incident energies, most of the ejected material comes from the first layer. Smith, R.; Garrision, D. E., Jr.; Garrision, B. J. In *Secondary Ion Mass Spectrometry SIMS VII*; Benninghoven, A., Evans, C. A., Jr., McKeegan, K. D., Storms, H. A., Werner, H. W., Eds.; John Wiley and Sons: New York, 1989.
(13) Gu, C.; Wysocki, V. H. *J. Am. Chem. Soc.* **1997**, *119*, 12010.
(14) Houssiau, L.; Graupe, M.; Colorado, R.; Kim, H. I.; Lee, T. R.; Perry, S. S.; Rabalais, J. W. *J. Chem. Phys.* **1998**, *109*, 9134.
(15) Wainhaus, S. B.; Lim, H. J.; Schultz, D. G.; Hanley, L. *J. Chem. Phys.* **1997**, *106*, 10329.
(16) Schultz, D. G.; Wainhaus, S. B.; Hanley, L.; deSainteClaire, P.; Hase, W. L. *J. Chem. Phys.* **1997**, *106*, 10337.
(17) Kane, T. E.; Somogyi, A.; Wysocki, V. H. *Org. Mass Spectron.* **1993**, *28*, 1665.
(18) Zamborini, F. P.; Campbell, J. K.; Crooks, R. M. *Langmuir* **1998**, *14*, 640.
(19) Cygan, M. T.; Dunbar, T. D.; Arnold, J. J.; Bumm, L. A.; Shedlock, N. F.; Burgin, T. P.; Jones, L.; Allara, D. L.; Tour, J. M.; Weiss, P. S. *J. Am. Chem. Soc.* **1998**, *120*, 2721.
(20) Xia, Y. N.; Whitesides, G. M. *Angew Chem., Int. Ed. Engl.* **1998**, *37*, 551.
(21) Eliadis, E. D.; Nuzzo, R. G.; Gewirth, A. A.; Alkire, R. C. *J. Electrochem. Soc.* **1997** *144*, 96.
(22) Ulman, A. *An Introduction to Ultrathin Organic Films; from Langmuir Blodgett to Self-Assembly*; Academic Press: New York, 1991.
(23) Ulman, A. *Chem. Rev.* **1996**, *96*, 1533.
(24) Murty, K. V. G. K.; Venkataramanan, M.; Pradeep, T. *Langmuir* **1998**, *14*, 5446.
(25) Chidsey, C. E. D.; Bertozzi, C. R.; Putvinski, T. M.; Mujsce, A. M. *J. Am. Chem. Soc.* **1990**, *112*, 4301.
(26) Winger, B. E.; Laue, H. J.; Horning, S. R.; Julian, R. K., Jr; Lammert, S. A.; Riederer, D. E., Jr.; Cooks, R. G. *Rev. Sci. Instrum.* **1992**, *63*, 5613.
(27) Cooks, R. G.; Rockwood, A. L. *Rapid Commun. Mass Spectrom.* **1991**, *5*, 93.
(28) Vincenti, M.; Cooks, R. G. *Org. Mass Spectrom.* **1988**, *23*, 317.
(29) Wainhaus, Samuel B.; Burroughs, John A.; Wu, Qinyuan; Hanley, Luke *Anal. Chem.* **1994**, *66*, 1038.
(30) *CRC Handbook of Chemistry and Physics*, 72nd ed.; CRC Press: Boca Raton, FL, 1991.
(31) Hayakawa, S.; Feng, B.; Cooks, R. G. *Int. J. Mass Spectrom. Ion Processes* **1997**, *167*, 525.
(32) Williams, E. R.; Jones, G. C., Jr.; Fang, L.; Zare, R. N.; Garrision, B. J.; Brenner, D. W. *J. Am. Chem. Soc.* **1992**, *114*, 3207.

(33) Winger, B. E.; Julian, R. K., Jr.; Cooks, R. G. *J. Am. Chem. Soc.* **1991**, *113*, 8967.
(34) Taylor, R. S.; Garrison, B. J. *Langmuir* **1995**, *11*, 1220.
(35) Yang, M. C.; Hwang, C. H.; Kang, H. *J. Chem. Phys.* **1997**, *107*, 2611.
(36) Willey, K. F.; Vorsa, V.; Braun, R. M.; Winograd, N. *Rapid Commun. Mass Spectrom.* **1998**, *12*, 1253.
(37) Riederer, D. E.; Chatterjee, R.; Rosencrance, S. W.; Postawa, Z.; Dunbar, T. D.; Allara, D. L.; Winograd, N. *J. Am. Chem. Soc.* **1997**, *119*, 8089.